Acta Crystallographica Section F
Structural Biology and Crystallization Communications
ISSN 1744-3091

Structure of HsaD, a steroid-degrading hydrolase, from *Mycobacterium tuberculosis*

Nathan Lack,[a] Edward D. Lowe,[b] Jie Liu,[c] Lindsay D. Eltis,[c] Martin E. M. Noble,[b] Edith Sim[a] and Isaac M. Westwood[a]*

[a]Department of Pharmacology, University of Oxford, Mansfield Road, Oxford OX1 3QT, England, [b]Laboratory of Molecular Biophysics, Department of Biochemistry, University of Oxford, South Parks Road, Oxford OX1 3QU, England, and [c]Department of Microbiology and Immunology, Life Sciences Institute, University of British Columbia, Vancouver BC V6T 1Z3, Canada

Correspondence e-mail: isaac.westwood@pharm.ox.ac.uk

Received 12 November 2007
Accepted 6 December 2007

PDB Reference: HsaD, 2vf2.

Tuberculosis is a major cause of death worldwide. Understanding of the pathogenicity of *Mycobacterium tuberculosis* has been advanced by gene analysis and has led to the identification of genes that are important for intracellular survival in macrophages. One of these genes encodes HsaD, a *meta*-cleavage product (MCP) hydrolase that catalyzes the hydrolytic cleavage of a carbon–carbon bond in cholesterol metabolism. This paper describes the production of HsaD as a recombinant protein and, following crystallization, the determination of its three-dimensional structure to 2.35 Å resolution by X-ray crystallography at the Diamond Light Source in Oxfordshire, England. To the authors' knowledge, this study constitutes the first report of a structure determined at the new synchrotron facility. The volume of the active-site cleft of the HsaD enzyme is more than double the corresponding active-site volumes of related MCP hydrolases involved in the catabolism of aromatic compounds, consistent with the specificity of HsaD for steroids such as cholesterol. Knowledge of the structure of the enzyme facilitates the design of inhibitors.

1. Introduction

HsaD is a member of the $\alpha\beta$-hydrolase superfamily, which includes the *meta*-cleavage product (MCP) hydrolases (Seah *et al.*, 2007). MCP hydrolases occur in the microbial pathways responsible for the aerobic catabolism of aromatic compounds, catalysing the hydrolytic cleavage of a carbon–carbon bond in the 2-hydroxy-6-oxo-dienoates that result from the *meta* cleavage of catechols by extradiol dioxygenases. HsaD from *Mycobacterium tuberculosis* H37Rv is a class I MCP hydrolase; this class includes enzymes involved in steroid and biphenyl catabolism (Seah *et al.*, 2007). Recent work has demonstrated that HsaD has high specificity for the steroid MCP 4,5-9,10-diseco-3-hydroxy-5,9,17-trioxoandrosta-1(10),2-diene-4-oic acid (4,9-DHSA) and is involved in cholesterol catabolism (Van der Geize *et al.*, 2007). The gene encoding HsaD in *M. tuberculosis* is found in an operon which was predicted (Payton *et al.*, 2001) and subsequently shown (Anderton *et al.*, 2006) to consist of genes encoding HsaA, HsaD, HsaC, HsaB (Van der Geize *et al.*, 2007), a hypothetical protein and an arylamine *N*-acetyltranferase (NAT), as shown in Fig. 1. The

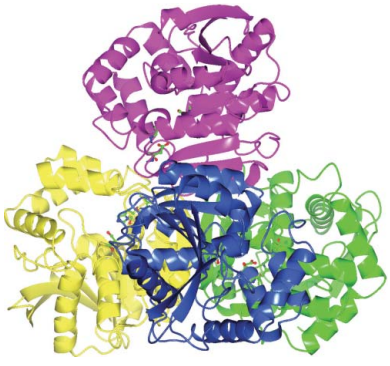

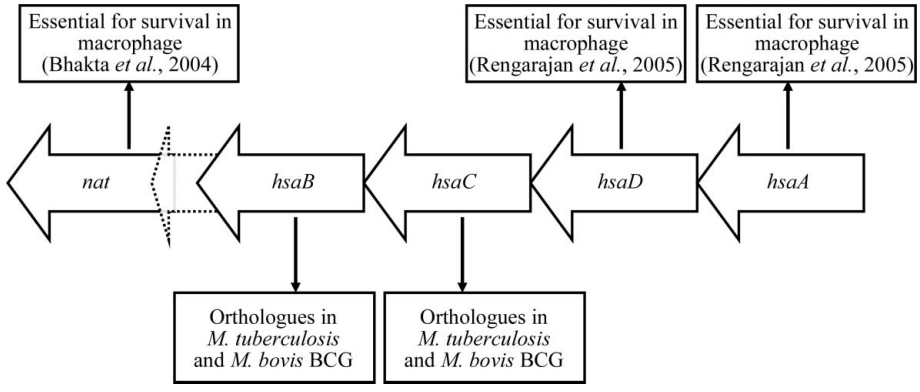

Figure 1
The *hsa* operon in *M. tuberculosis* and *M. bovis* BCG. The accession numbers for the genes in *M. tuberculosis* H37Rv, ordered from right to left, are *Rv3570c*, *Rv3569c*, *Rv3568c*, *Rv3567c*, *Rv3566A* and *Rv3566c*. The corresponding genes in *M. bovis* BCG have accession numbers *Mb3601c*, *Mb3600c*, *Mb3599c*, *Mb3598c*, *Mb3597c* and *Mb3596c*.

nat gene has been shown to be required for intracellular survival of the *M. tuberculosis* model organism *M. bovis* BCG inside macrophage cells (Bhakta *et al.*, 2004). The phenotype following ablation of the *nat* gene in *M. bovis* BCG was mimicked by growing the wild-type organism in the presence of a putative substrate of HsaC to act as a competitive inhibitor of this enzyme (Anderton *et al.*, 2006). Large-scale transposon-mutagenesis studies have suggested that the genes encoding HsaA and HsaD are also essential for intracellular survival of *M. tuberculosis* in human macrophages (Rengarajan *et al.*, 2005). Recent work has demonstrated that this operon is part of a larger regulon that is involved in lipid metabolism (Kendall *et al.*, 2007). Therefore, the enzymes encoded by the genes in this operon are important for understanding the biology of *M. tuberculosis* and also represent potential therapeutic targets.

In this paper, we report the 2.35 Å resolution structure of HsaD from *M. tuberculosis* solved by X-ray crystallography at the Diamond Light Source synchrotron.

2. Materials and methods

2.1. Production and purification of HsaD

The *HsaD* open reading frame was cloned from *M. tuberculosis* strain H37Rv into the expression vector pVLT31 with a 20-amino-acid N-terminal hexahistidine tag (amino-acid sequence MGSSHHHHHHSSGLVPR). The expression host used was *Pseudomonas putida* KT4224. Heterologous expression in LB medium at 303 K gave a typical yield of 15 mg HsaD protein per litre of bacterial culture after purification by immobilized nickel-ion affinity chromatography. The N-terminal hexahistidine tag could not be removed from the recombinant protein by thrombin cleavage. Details of the cloning, expression and protein purification will be published elsewhere.

2.2. Crystallization and structure solution

Purified recombinant HsaD protein (in 100 m*M* sodium phosphate pH 7.4) was concentrated to 10 mg ml^{-1} with an Amicon ultracentrifugation concentrator (Millipore, Watford, Hertfordshire). The crystals described in this paper were grown at 292 K by the sitting-drop vapour-diffusion method. For crystallization, 150 nl concentrated HsaD solution was mixed with 150 nl precipitant [30%(*w*/*v*) PEG 3000, 0.1 *M* CHES pH 9.5] and the volume of precipitant in the reservoir was 100 µl. Crystals typically grew within 3–5 d.

Crystals were briefly transferred to a cryoprotectant solution [a 3:1(*v*:*v*) mixture of precipitant and glycerol] prior to flash-freezing in liquid nitrogen. Diffraction data were collected from one plate-shaped crystal of approximate dimensions 50 × 50 × 10 µm at beamline IO4 at the Diamond Light Source, Oxfordshire, England. Data from 178 images (oscillation range 0.5°) were indexed and integrated with *MOSFLM* (Leslie, 1992) and scaled with *SCALA* (Evans, 2006). Initial phases were determined by molecular repla-

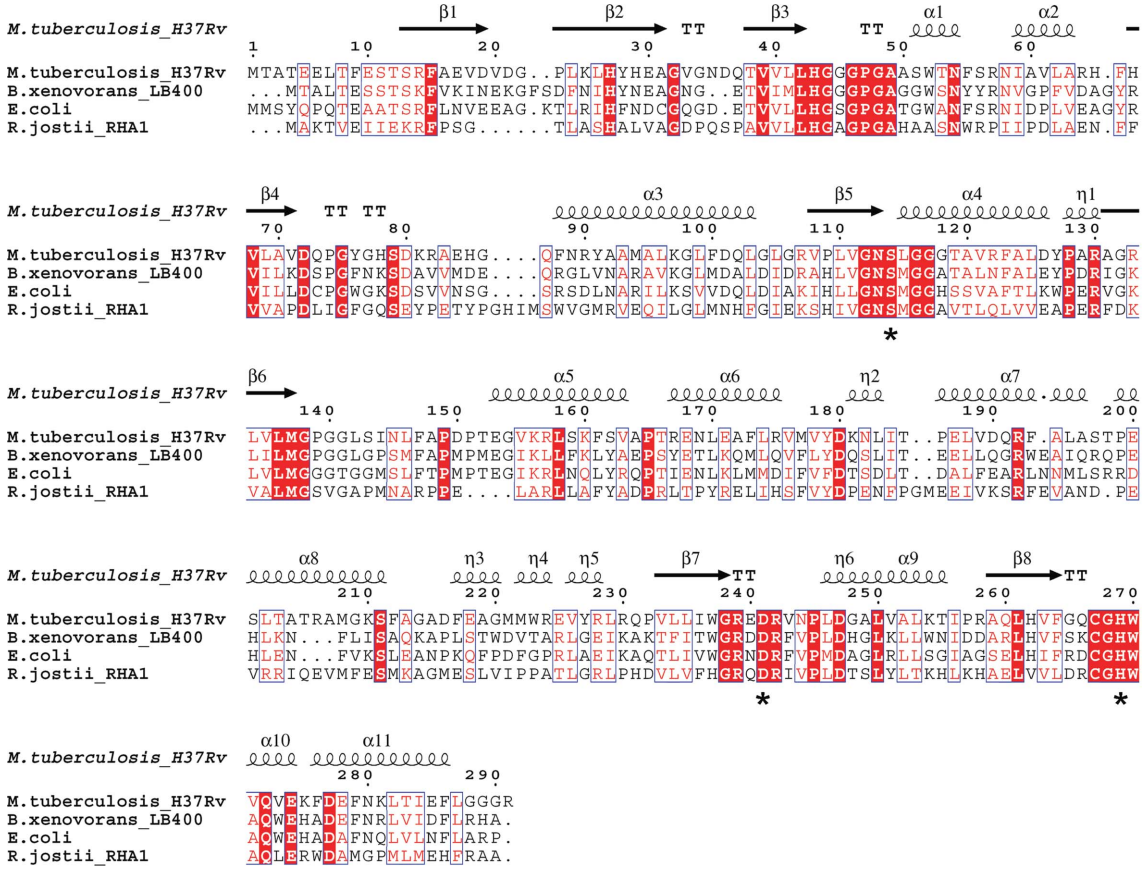

Figure 2
Sequence alignment of the HsaD protein from *M. tuberculosis* with BphDs from *B. xenovorans* (PDB code 2og1) and *R. jostii* RHA1 (PDB code 1c4x) and MphC from *E. coli* (PDB code 1u2e). The structure of HsaD from *M. tuberculosis* was used to generate the structural annotations. The catalytic triad residues Ser114, His269 and Asp241 (*M. tuberculosis* HsaD numbering) are indicated by black stars. The alignment was performed with *ClustalW* (Chenna *et al.*, 2003) and the figure was prepared with *ESPRIPT* (Gouet *et al.*, 1999).

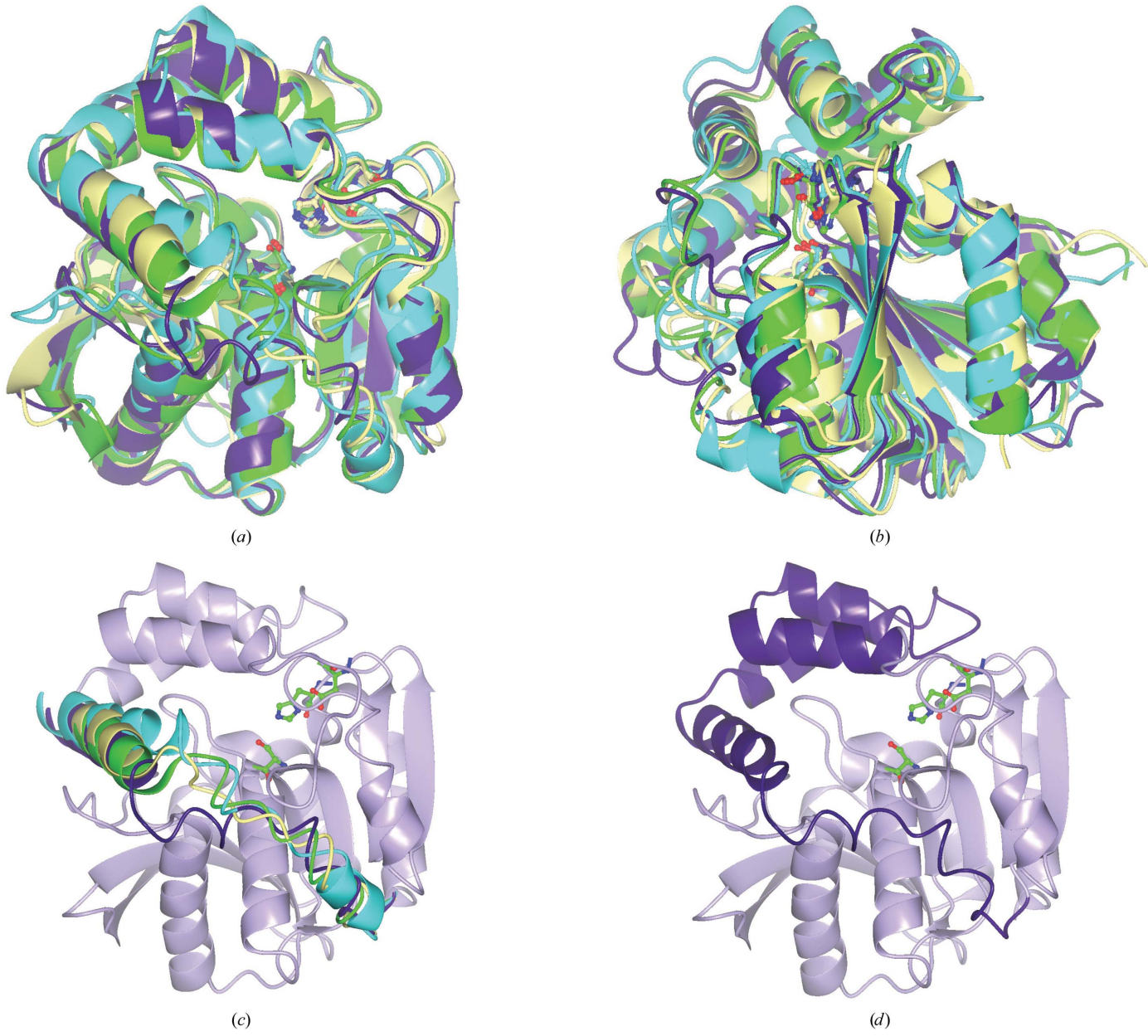

Figure 3
(*a*, *b*) Orthogonal views of the ribbon structurs of HsaD from *M. tuberculosis* (PDB code 2vf2, purple) aligned with those of the BphD enzymes from *B. xenovorans* LB400 (PDB code 2og1, green) and *R. jostii* RHA1 (PDB code 1c4x, cyan) and of MphC from *E. coli* (PDB code 1u2e, yellow). (*c*) A view of the overlay highlighting the region correlating to amino acids 199–232 in *M. tuberculosis* HsaD. (*d*) A view highlighting the α-helical lid domain of *M. tuberculosis* HsaD. The structural alignments were performed by secondary-structure matching (*SSM*) in *CCP4mg* (Krissinel & Henrick, 2004; Potterton *et al.*, 2004).

cement with the program *Phaser* (Read, 2001) by using an ensemble of the MCP hydrolases from *Burkholderia xenovorans* LB400 (PDB code 2og1; Horsman *et al.*, 2006) and *Rhodococcus jostii* RHA1[1] (PDB code 1c4x; Nandhagopal *et al.*, 1997) as search templates, with nonconserved residues truncated to the C^{β} atom with the program *CHAINSAW* (Schwarzenbacher *et al.*, 2004). Initial model building was performed with *ARP*/*wARP* (Morris *et al.*, 2003) and was followed by iterative cycles of manual building with *Coot* (Emsley & Cowtan, 2004), refinement with *REFMAC* (Murshudov *et al.*, 1997) or *phenix.refine* (Adams *et al.*, 2002) and model-quality checking with *MOLPROBITY* (Davis *et al.*, 2007). The protein model was solvated and the waters checked with *phenix.refine* and *Coot*. The stereochemical quality of the final model was assessed with the programs *MOLPROBITY* and *PROCHECK* (Laskowski *et al.*, 1993). Data-collection and refinement statistics are shown in Table 1.

[1] Formerly *Rhodococcus* sp. RHA1; the species was recently identified by A. L. Jones and M. Goodfellow (personal communication).

3. Results and discussion

The recombinant *M. tuberculosis* HsaD protein was produced, purified and crystallized as described in §2. A summary of the data-collection and refinement statistics is presented in Table 1. The asymmetric unit of the *M. tuberculosis* HsaD crystal structure consists of two chains, each of 284 amino-acid residues (Leu7–Gly290). The electron density was not sufficiently well resolved to model the 26

N-terminal residues, which include the 20-amino-acid hexahistidine affinity tag used for protein purification, or the C-terminal arginine residue.

The *M. tuberculosis* HsaD enzyme shares only modest amino-acid sequence identity with other MCP hydrolases, including MhpC from *Escherichia coli* (Dunn *et al.*, 2005) and the BphD enzymes from *B. xenovorans* LB400 (Horsman *et al.*, 2006) and *R. jostii* RHA1 (Nandhagopal *et al.*, 1997), as shown in Table 2. Despite these modest sequence identities, the *M. tuberculosis* HsaD protein adopts a three-dimensional fold which is highly similar to those of these known MCP hydrolases. The root-mean-square deviations of the C^{α} backbone atoms between *M. tuberculosis* HsaD and each of these three MCP hydrolases are given in Table 2. Fig. 2 shows a sequence alignment of these four proteins; an overlay of their three-dimensional structures is shown in Fig. 3.

In all four crystal structures shown in Fig. 3 an α-helical lid domain (α5–η5, amino acids 153–232) is encompassed by an α/β-domain. The α/β-domain is made up of a central β-sheet consisting of three anti-parallel strands followed by five parallel strands (from the N-terminus to the C-terminus), surrounded by five α-helices. The active sites of MCP hydrolases are composed of a polar portion (P) and a nonpolar portion (NP) (Seah *et al.*, 2007), with a well conserved central catalytic triad of residues, Ser114, His269 and Asp241 (*M. tuberculosis* HsaD numbering). Of these three residues, only the histidine is conserved throughout all known $\alpha\beta$-hydrolases and recent studies have explored the mechanistic role of the active-site histidine residue of BphD from *B. xenovorans* (Horsman *et al.*, 2007). The NP subsite of *M. tuberculosis* HsaD appears to be the entrance to the active-site cleft, in contrast to the proposed active-site entrance (P subsite) of *R. jostii* RHA1 BphD (Nandhagopal *et al.*, 2001). One key difference in the three-dimensional fold of *M. tuberculosis* HsaD relative to these other three MCP hydrolases is the location of amino-acid residues 213–224 (HsaD numbering), which stretches from the C-terminus of α8 to the end of η4 (Fig. 3) and forms one edge of the NP subsite. The corresponding regions in the other MCP hydrolases are closer to the catalytic triad, resulting in a significantly smaller NP subsite in these proteins relative to *M. tuberculosis* HsaD (Fig. 4). The calculated volume of the NP portion of the active-site cavity of *M. tuberculosis* HsaD (~2100 Å^3) was approximately twofold larger than the corresponding cavity in *B. xenovorans* BphD (~1200 Å^3) and around fourfold larger than the cavities in the other two MCP hydrolases shown in Fig. 4 (~500 Å^3), as determined from the PDB files using the program *VOIDOO* (Kleywegt & Jones, 1994). This large nonpolar portion of the active site is consistent with the role of *M. tuberculosis* HsaD in hydrolysis of the cholesterol MCP 4,9-DHSA (Van der Geize *et al.*, 2007).

The *M. tuberculosis* HsaD protein structure was found to adopt a tetrameric assembly in the protein crystal, as shown in Fig. 5. This tetrahedral structure may be described as a dimer of dimers in which the two monomers in each dimer (green/yellow and blue/magenta in

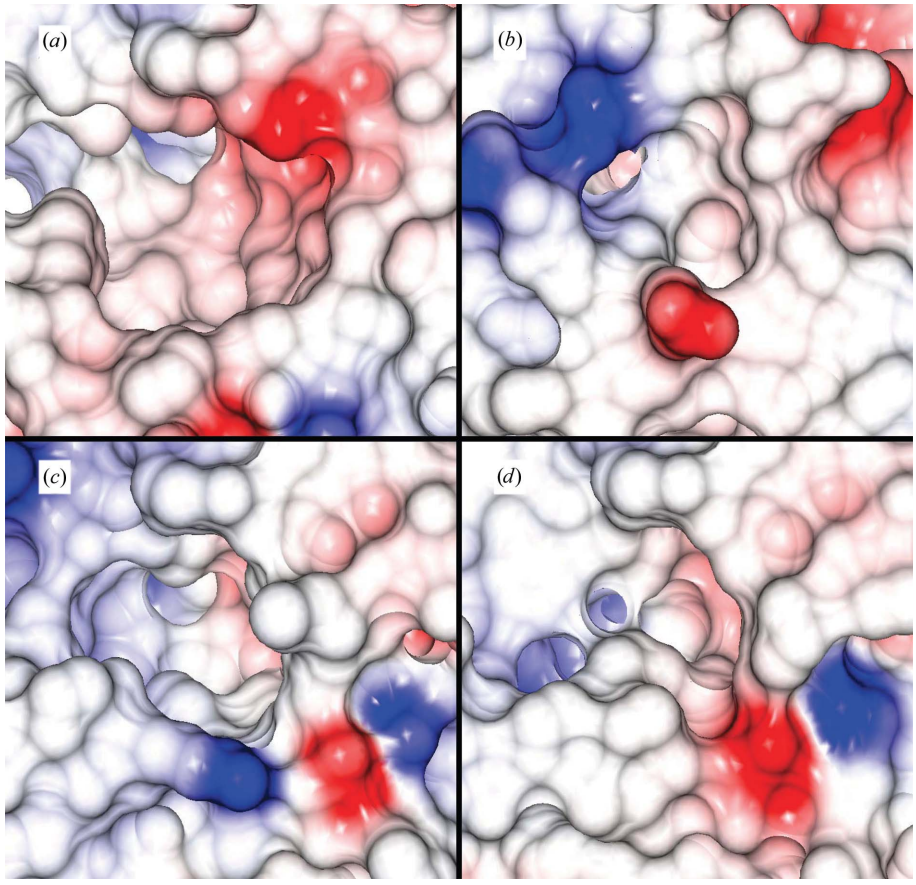

Figure 4
Comparison of the nonpolar (NP) portion of the active-site surfaces of (*a*) *M. tuberculosis* HsaD (PDB code 2vf2), (*b*) BphD from *R. jostii* RHA1 (PDB code 1c4x), (*c*) MphC from *E. coli* (PDB code 1u2e) and (*d*) BphD from *B. xenovorans* (PDB code 2og1). The surfaces are coloured by electrostatic potential. The surfaces were calculated for the overlaid structures (Fig. 3) and the figure was prepared with *CCP4mg*.

Table 1
Summary of data-collection and refinement statistics.

Values in parentheses are for the highest resolution shell.

Space group	$I2_12_12_1$
Unit-cell parameters	a = 82.36, b = 82.46, c = 194.67, $\alpha = \beta = \gamma = 90$
Data-collection statistics	
Wavelength (Å)	0.96800
Resolution (Å)	32.4–2.35 (2.48–2.35)
No. of unique reflections	24657 (3312)
R_{merge}†	0.075 (0.50)
$I/\sigma(I)$	7.9 (1.5)
Completeness (%)	96.7 (93.6)
Redundancy	3.4 (3.4)
Refinement and model statistics	
Resolution (Å)	32.4–2.35 (2.40–2.35)
No. reflections used (work + test)	24657
R_{work}‡	0.212 (0.305)
R_{free}‡	0.233 (0.294)
No. of residues (chain A/chain B)	284/284
No. of water molecules	208
Additional molecules	3 glycerol, 2 sulfate
Total No. of atoms	4624
R.m.s.d. bond lengths (Å)	0.015
R.m.s.d. bond angles (°)	0.81
Mean B factor (Å^2)	54.1
Ramachandran statistics (%)	
Core region	88.4
Additional allowed region	11.2
Generously allowed	0.4
Disallowed	0.0

† $R_{merge} = \sum_{hkl}\sum_i |I_i(hkl) - \overline{I(hkl)}|/\sum_{hkl}\sum_i I_i(hkl)$, where $I_i(hkl)$ is the intensity of the ith observation of unique reflection h. ‡ R_{work} and $R_{free} = \sum_h ||F_o(h)| - |F_c(h)||/\sum_h |F_o(h)|$ for the working set and test set (5%) of reflections, where $F_o(h)$ and $F_c(h)$ are the observed and calculated structure-factor amplitudes for reflection h.

Fig. 5) are arranged such that an extended 16-strand β-sheet is formed. This tetrahedral assembly was predicted to be stable in solution using the PISA web service at the European Bioinformatics Institute (Krissinel & Henrick, 2007). The active site of each monomer appears to be distinct and the entrance to each active site (*e.g.* Fig. 5*a*) is in close proximity to the monomer–monomer β-sheet interface of the opposite dimer (*e.g.* B–B'). It may therefore be possible for particularly large or long-chain substrates bound at the active site to also interact with residues on the opposite dimer. The equivalent multimeric assemblies of the MCP hydrolases from *B. xenovorans* (PDB code 2og1) and *E. coli* (PDB code 1u2e) have also been described (Dunn *et al.*, 2005; Horsman *et al.*, 2006).

Table 2
Comparison of the sequence identities and three-dimensional similarity of four MCP hydrolases.

Enzyme	PDB code	Sequence identity to HsaD (%)	R.m.s. deviation of C$^\alpha$ atoms *versus* HsaD (Å)	Reference
MhpC, *E. coli*	1u2e	36	1.51	Dunn *et al.* (2005)
BphD, *B. xenovorans*	2og1	44	1.43	Horsman *et al.* (2006)
BphD, *R. jostii* RHA1	1c4x	29	1.71	Nandhagopal *et al.* (1997)

In summary, the three-dimensional structure of the HsaD protein from *M. tuberculosis* has been determined by X-ray crystallography at the Diamond Light Source in Oxfordshire, England. The structure shows very high overall similarity to those of other known MCP hydrolases, with the notable exception of one region bounding the active-site pocket. The result of this difference is a larger active site relative to the previously described MCP hydrolases, which is consistent with the substrate specificity of HsaD from *M. tuberculosis*. The gene encoding HsaD has previously been shown to be essential for the survival of *M. tuberculosis* inside macrophages and therefore this structure provides a basis for rational ligand design, which will be important both for understanding the biology of *M. tuberculosis* and for the development of novel antituberculosis agents.

The authors thank the Wellcome Trust for financial support. NL is in receipt of a Canadian National Scholarship (Linacre College, University of Oxford) and a Natural Sciences and Engineering

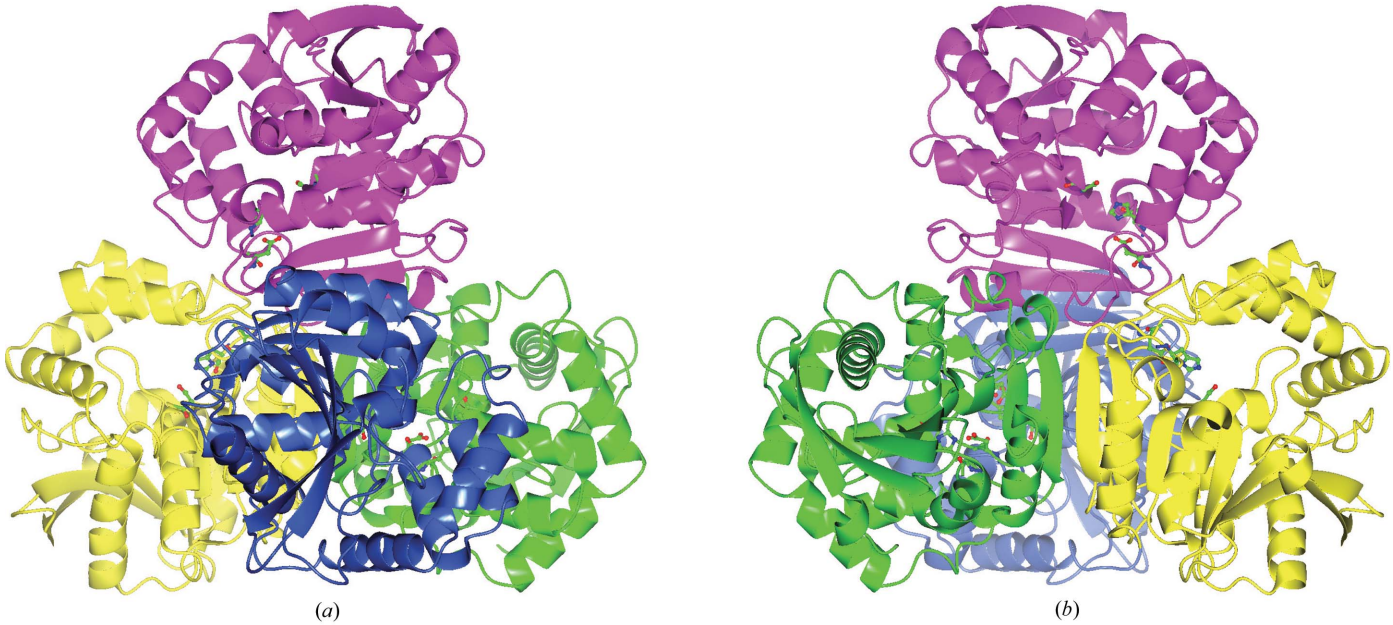

Figure 5
The predicted tetrahedral tetrameric assembly of *M. tuberculosis* HsaD in solution. The molecular assembly was predicted using the Protein Interfaces, Surfaces and Assemblies service (PISA) at the European Bioinformatics Institute (http://www.ebi.ac.uk/msd-srv/prot_int/pistart.html; Krissinel & Henrick, 2007). The assembly may be described as a dimer of dimers in which the monomers coloured green and yellow form one dimer and the monomers coloured blue and magenta form the second dimer. The view in (*b*) was generated by rotating view (*a*) by 180° around the y axis. The figure was prepared with *CCP4mg*.

Research Council of Canada (NSERC) Scholarship. LDE acknowledges support from the Canadian Institutes for Health Research (CIHR). The authors also thank Sanjib Bhakta (Birkbeck College, London) for *M. tuberculosis* genomic DNA and the beamline scientists at IO4 of the Diamond Light Source for technical support.

References

Adams, P. D., Grosse-Kunstleve, R. W., Hung, L.-W., Ioerger, T. R., McCoy, A. J., Moriarty, N. W., Read, R. J., Sacchettini, J. C., Sauter, N. K. & Terwilliger, T. C. (2002). *Acta Cryst.* D**58**, 1948–1954.
Anderton, M. C., Bhakta, S., Besra, G. S., Jeavons, P., Eltis, L. D. & Sim, E. (2006). *Mol. Microbiol.* **59**, 181–192.
Bhakta, S., Besra, G. S., Upton, A. M., Parish, T., Sholto-Douglas-Vernon, C., Gibson, K. J. C., Knutton, S., Gordon, S., daSilva, R. P., Anderton, M. C. & Sim, E. (2004). *J. Exp. Med.* **199**, 1191–1199.
Chenna, R., Sugawara, H., Koike, T., Lopez, R., Gibson, T. J., Higgins, D. G. & Thompson, J. D. (2003). *Nucleic Acids Res.* **31**, 3497–3500.
Davis, I. W., Leaver-Fay, A., Chen, V. B., Block, J. N., Kapral, G. J., Wang, X., Murray, L. W., Arendall, W. B. III, Snoeyink, J., Richardson, J. S. & Richardson, D. C. (2007). *Nucleic Acids Res.* **35**, W375–W383.
Dunn, G., Montgomery, M. G., Mohammed, F., Coker, A., Cooper, J. B., Robertson, T., Garcia, J. L., Bugg, T. D. & Wood, S. P. (2005). *J. Mol. Biol.* **346**, 253–265.
Emsley, P. & Cowtan, K. (2004). *Acta Cryst.* D**60**, 2126–2132.
Evans, P. (2006). *Acta Cryst.* D**62**, 72–82.
Gouet, P., Courcelle, E., Stuart, D. I. & Metoz, F. (1999). *Bioinformatics*, **15**, 305–308.
Horsman, G. P., Bhowmik, S., Seah, S. Y., Kumar, P., Bolin, J. T. & Eltis, L. D. (2007). *J. Biol. Chem.* **282**, 19894–19904.
Horsman, G. P., Ke, J., Dai, S., Seah, S. Y., Bolin, J. T. & Eltis, L. D. (2006). *Biochemistry*, **45**, 11071–11086.
Kendall, S. L., Withers, M., Soffair, C. N., Moreland, N. J., Gurcha, S., Sidders, B., Frita, R., Ten Bokum, A., Besra, G. S., Lott, J. S. & Stoker, N. G. (2007). *Mol. Microbiol.* **65**, 684–699.
Kleywegt, G. J. & Jones, T. A. (1994). *Acta Cryst.* D**50**, 178–185.
Krissinel, E. & Henrick, K. (2004). *Acta Cryst.* D**60**, 2256–2268.
Krissinel, E. & Henrick, K. (2007). *J. Mol. Biol.* **372**, 774–797.
Laskowski, R. A., MacArthur, M. W., Moss, D. S. & Thornton, J. M. (1993). *J. Appl. Cryst.* **26**, 283–291.
Leslie, A. G. W. (1992). *Jnt CCP4/ESF–EACBM Newsl. Protein Crystallogr.* **26**.
Morris, R. J., Perrakis, A. & Lamzin, V. S. (2003). *Methods Enzymol.* **374**, 229–244.
Murshudov, G. N., Vagin, A. A. & Dodson, E. J. (1997). *Acta Cryst.* D**53**, 240–255.
Nandhagopal, N., Senda, T., Hatta, T., Yamada, A., Masai, E., Fukuda, M. & Mitsui, Y. (1997). *Proc. Jpn Acad. Ser. B*, **73**, 154–157.
Nandhagopal, N., Yamada, A., Hatta, T., Masai, E., Fukuda, M., Mitsui, Y. & Senda, T. (2001). *J. Mol. Biol.* **309**, 1139–1151.
Payton, M., Mushtaq, A., Yu, T. W., Wu, L. J., Sinclair, J. & Sim, E. (2001). *Microbiology*, **147**, 1137–1147.
Potterton, L., McNicholas, S., Krissinel, E., Gruber, J., Cowtan, K., Emsley, P., Murshudov, G. N., Cohen, S., Perrakis, A. & Noble, M. (2004). *Acta Cryst.* D**60**, 2288–2294.
Read, R. J. (2001). *Acta Cryst.* D**57**, 1373–1382.
Rengarajan, J., Bloom, B. R. & Rubin, E. J. (2005). *Proc. Natl Acad. Sci. USA*, **102**, 8327–8332.
Schwarzenbacher, R., Godzik, A., Grzechnik, S. K. & Jaroszewski, L. (2004). *Acta Cryst.* D**60**, 1229–1236.
Seah, S. Y., Ke, J., Denis, G., Horsman, G. P., Fortin, P. D., Whiting, C. J. & Eltis, L. D. (2007). *J. Bacteriol.* **189**, 4038–4045.
Van der Geize, R., Heuser, T., Yam, K., Wilbrink, M., Hara, H., Anderton, M. C., Sim, E., Dijkhuizen, L., Davies, J., Mohn, W. & Eltis, L. D. (2007). *Proc. Natl Acad. Sci. USA*, **104**, 1947–1952.